Proceedings of the 5th International Conference of Fluid Flow, Heat and Mass Transfer (FFHMT'18)
Niagara Falls, Canada – June 7 – 9, 2018
Paper No. 180
DOI: 10.11159/ffhmt18.180

A Computational Analysis of Gas Jet Flow Effects on Liquid Aspiration in the Collison Nebulizer

James Q. Feng
Optomec, Inc.
2575 University Ave., #135, St. Paul, MN 55114, USA
jfeng@optomec.com

Abstract - Pneumatic nebulizers (as variations based on the Collison nebulizer) have been widely used for producing fine aerosol droplets from a liquid material. The basic working principle of those nebulizers has been qualitatively described as utilization of the negative pressure associated with an expanding gas jet to syphon liquid into the jet stream, then to blow and shear into liquid sheets, filaments, and eventually droplets. Detailed quantitative analysis based on fluid mechanics theory is desirable, to gain in-depth understanding of the liquid aspiration mechanism among other aspects of the Collison nebulizer behaviour. The purpose of present work is to investigate the nature of negative pressure distribution associated with compressible gas jet flow in the Collison nebulizer by a computational fluid dynamics (CFD) analysis, using an OpenFOAM® compressible flow solver. The value of the negative pressure associated with a gas jet flow is examined by varying geometric parameters of the jet expansion channel adjacent to the outlet of jet orifice. Such an analysis can provide valuable insights into fundamental mechanisms for liquid aspiration, helpful for designing improved pneumatic atomizer in the Aerosol Jet® direct-write system for micro-feature, high-aspect-ratio material deposition.

Keywords**:** Collison Nebulizer, Compressible Gas Jet Flow, Liquid Aspiration, Pneumatic Atomization.

1. Introduction

The original motivation to develop pneumatic nebulizers was for producing medical aerosols in the inhalation therapy [1]. Among many variations, the Collison nebulizer (introduced by W. E. Collison) has been the most representative one, widely used in applications extended even beyond therapeutic inhalers. For example, the Aerosol Jet® direct-write system typically includes a pneumatic atomizer with similar configuration as the Collison nebulizer, for producing aerosol droplets of functional ink materials in the size range of 1 to 5 μm [2, 3]. This type of pneumatic nebulizer is capable of effectively atomizing liquids much more viscous than the usual therapeutic ones, enabling Aerosol Jet® to print inks with high concentrations of functional materials. To further improve the pneumatic atomizer in Aerosol Jet® systems, it is important to understand the fluid dynamic effects of various parameters involved in the atomizer design.

Despite its wide usage in a variety of applications, the technical details about fluid dynamic behavior of the Collison nebulizer can rarely be found in the current literature. The only noticeable paper is that published by May in 1973 [1], providing some design details and various experimental data through scientific measurements. Although there were a few later publications [4, 5] providing more data regarding functional aspects of various pneumatic (or "air-jet") nebulizers, the description of basic working principle remained at the level of qualitative hand-waiving.

Here in this work, a computational fluid dynamics (CFD) analysis is conducted to investigate effects of atomizer geometric parameters on the compressible gas jet flow behavior based on a Collison nebulizer configuration. The results can provide valuable insights into the process of liquid aspiration, which plays a key role in the Collison nebulizer performance, for designing improved pneumatic atomizers for the Aerosol Jet® systems.

2. Problem Description

2.1. Working Principle of the Collison Nebulizer

As described by May [1], the Collison nebulizer (schematically shown in Fig. 1) consists of a small jet orifice that produces a jet around sonic speed as compressed gas flows through it. Such a jet formed from compressed gas would expand in the jet expansion channel downstream of the jet orifice, creating a reduction of local static pressure (or "negative pressure") to suck liquid ink through the ink syphon tube. Thus, the ink syphoned into the jet stream region can then form

liquid sheets, filaments, and droplets under the strong shear of high-speed jet flow. No active liquid pump is used here, remarkably.

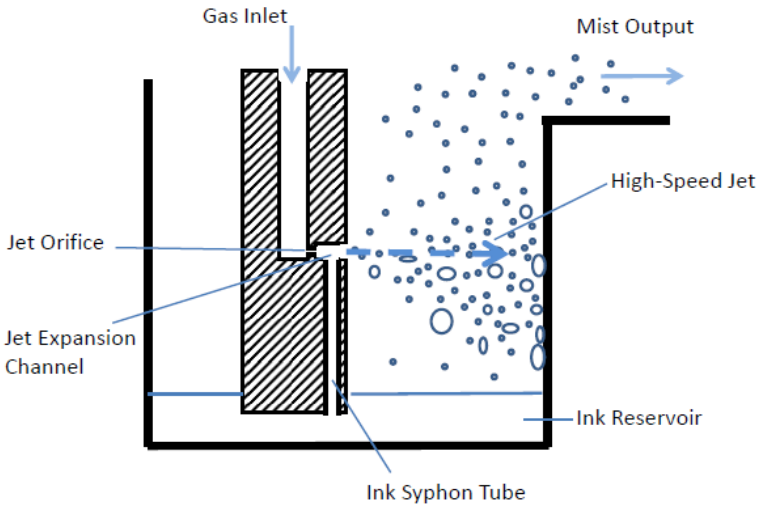

Fig. 1: Schematic of a typical configuration of the Collison nebulizer.

However, the liquid droplets produced by such a blowing gas jet often have a very wide size distribution. To remove droplets larger than 5 μm or so, the droplets carried by the jet flow are directed toward the wall of nebulizer chamber, where large droplets with sufficient mass are blown onto by inertial impaction. Only a small fraction (typically < 0.1%) of the liquid syphoned into jet stream can become fine enough droplets (e.g., < 5 μm) to escape impact and be carried by the gas flow as the output mist [1].

Because more than 99.9% of the liquid ink going through the atomization process might be cycled back to the ink reservoir, the liquid aspiration rate through the ink syphon tube is expected to substantially influence the output mist density of the nebulizer. Sufficient liquid aspiration rate requires sufficient negative pressure in the jet expansion channel. For a given aspiration rate, an ink with higher viscosity needs stronger negative pressure. Thus, the magnitude of negative pressure generated in the jet expansion channel by compressible gas jet flow becomes the subject of study in this paper.

2.2. Atomization Behaviour of the Collison Nebulizer

Many applications desire high liquid mass output from the nebulizer, which is probably why the Collison nebulizer typically operates with a gas flow rate Q > 2000 sccm (per jet), through a jet orifice typically of diameter D = 0.35 mm. It has commonly observed that the liquid mass density in output mist (also known as the mist density) decreases with the gas flow rate, although the liquid mass output still increases for Q > 2000 sccm [1]. This fact suggests that beyond 2000 sccm the increase of liquid atomization rate cannot catch up the increase of gas flow rate.

In contrast, for Aerosol Jet® direct-write applications, the output mist density generated from its (Collison-type) pneumatic atomizer is much more relevant to the desired high printing throughput. Depending on ink materials, it has been found more often than not that the peak mist density is obtained at a gas flow rate around Q = 1200 sccm; further increasing the gas flow rate rather yields lower mist density. With more careful experimentations, most inks for Aerosol Jet® printing are found to yield mist output at a gas flow rate greater than Q = 600 sccm.

In the standard Collison nebulizer configuration, the atomization jet (as well as the jet expansion channel) is located about h = 20 mm above the liquid level in the ink reservoir (cf. Fig. 1). To bring ink through its syphon tube from the reservoir up to the jet stream for atomization, the pressure in jet expansion channel must be reduced to a level at least enough to overcome the hydrostatic pressure $\rho_{ink}\, g\, h$ with ρ_{ink} denoting the ink density and g (= 9.81 m s^{-2}) the gravitational acceleration. Most metal nanoparticle inks for Aerosol Jet® in printing electronic devices often have ρ_{ink} about 2 g/cc. Thus the hydrostatic pressure may be estimated as about 400 Pa. In other words, the reduction of pressure (also known as the "negative pressure") in jet expansion channel from that in the atomizer chamber (which is usually very close to the

ambient value, e.g., 10^5 Pa) must be greater than 400 Pa (plus or minus about 100 Pa due to the capillary effect depending on the contact angle and surface tension of the ink) at a gas flow rate of Q = 600 sccm.

When the volumetric flow rate Q of compressible gas flow is measured in units of "standard cubic centimeters per minute" (sccm), the actual volumetric flow rate varies with temperature but the mass flow rate remains as a constant. Thus, the value of $\rho U = 4\ \rho_s\ Q\ /\ (\pi D^2)$ is a constant for given Q and D, with ρ and ρ_s denoting the actual density of gas and that under standard conditions at T_s = 273 K and $P_s = 10^5$ Pa, e.g., $\rho_s = P_s\ /\ (R\ T_s)$ = 1.276 kg/m^3 for dry air (which is about the same as the dry nitrogen typically used as the inert carrier gas in Aerosol Jet® systems). The value of the jet Reynolds number $Re = \rho\ U\ D\ /\ \mu$ can be calculated as 1.464 Q / D with Q in units of sccm and D in millimeters assuming the dynamic viscosity of gas μ = 1.85 x 10^{-5} kg m^{-1} s^{-1} (at T = 300 K). Hence Re = 5018 with Q = 1200 sccm and D = 0.35 mm, while Re = 2509 for Q = 600 sccm.

2.3. The CFD Model

The mathematical model considered here is for fluid dynamics simulation of a compressible gas flowing from an inlet channel through a small jet orifice into a jet expansion channel of larger diameter and then into a much large atomization chamber with a solid wall at its end. For simplicity without loss of the essence of the problem, all the involved channels are arranged concentrically such that the computational domain becomes axisymmetric (with negligible effect of gravity in such a microscale gas flow).

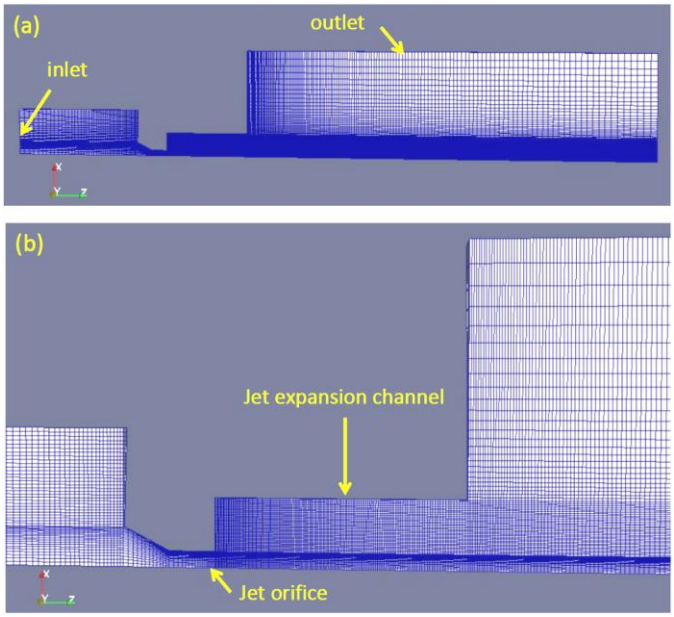

Fig. 2: (a) Complete, and (b) regional details of the computational domain with a wedge type mesh for axisymmetric problem, generated with the *blockMesh* utility.

As a nominal model setting, the jet orifice has a diameter of D = 0.35 mm and the diameter and length of jet expansion channel are D_e = 1.5 mm and L_e = 2.7 mm, to be consistent with the standard Collison nebulizer design [1]. To complete model construction, the computational domain also contains an entrance tube of 3 mm diameter upstream of the jet orifice and a large cylindrical chamber with diameter of 7 mm and length of 14 mm downstream of the jet expansion channel (as shown in Fig. 2). Except the axis of symmetry, the inlet patch at the upstream end of the entrance tube and the outlet patch as the cylindrical side of the large atomization chamber, all other physical boundaries of the computational domain are treated as solid walls.

Among several choices, the steady compressible flow solver known as *rhoSimpleFoam*, available in the OpenFOAM® CFD Toolbox v.2.4.0 [6], is used for computing solutions of the Navier-Stokes equation system (which includes equations for conservations of mass, momentum, and energy, governing the flow of a fluid described by the ideal gas law and

Fourier's law of heat conduction with Sutherland's law for dynamic viscosity). This solver also contains a variety of turbulence models. The 3D meshing utility *blockMesh*, included in the OpenFOAM® package, is used to generate mesh according to the computational domain (in Fig. 2).

The boundary conditions for flow velocity U, pressure p, and temperature T at solid walls are *fixedValue* (for U = 0), *zeroGradient* (for p), and *fixedValue* (T = 300K), at inlet *flowRateInletVelocity* (for U with a specified mass flow rate), *zeroGradient* (for p), and *fixedValue* (T = 300K), and at outlet *pressureInletOuletVelocity* (for U), *fixedValue* (for $p = 10^5$ Pa), and *zeroGradient* (for T), respectively.

Based on estimated values of the jet Reynolds number (e.g., ~2500 at Q = 600 sccm, etc.), the free jet flow out of the small orifice (with D = 0.35 mm) is expected to be turbulent [7--9]. Thus some kind of turbulence model should be included in the present CFD model. For lack of better knowledge, a common k-ε model is used here based on Reynolds Averaged Navier-Stokes (RANS) equations, which is (among others) available in the *rhoSimpleFoam* solver.

3. Results

It is usually difficult to obtain converged solutions by running the *rhoSimpleFoam* solver from a simple default initial condition. In the present work, the corresponding transient flow solver known as *rhoPimpleFoam*, also available in OpenFOAM®, is used for computing compressible flow solutions over certain time span to supply more reasonable initial conditions for the *rhoSimpleFoam* solver to compute the steady-state solutions.

3.1. The Nominal Case

For the nominal case with jet orifice of D = 0.35 mm with a jet expansion channel of D_e = 1.5 mm and L_e = 2.7 mm, the computed results of gas flow field in terms velocity magnitude $|U|$, pressure p, gas density ρ, and temperature T with a gas flow rate of Q = 1200 sccm are shown in Fig. 3. At the exit of the jet orifice, the jet velocity can approach 246 m/s, corresponding to a Mach number Ma = 0.746. Then, the jet expands with velocity decreasing as it moves forward. A significant region of negative pressure ΔP ~1524 Pa indeed appears in the jet expansion channel, providing the syphoning effect for liquid aspiration. Somehow the pressure field does not exhibit similar distribution structure as that of the flow velocity. The lowest pressure zone does not coincide with that of highest velocity as anticipated from Bernoulli's principle. The peak value of gas density (ρ = 1.65 kg/m^3) upstream to the jet orifice matches that calculated for $p = 1.425 \times 10^5$ Pa and T = 300 K according to the ideal gas law for dry air (i.e., 1.655 kg/m^3). The value minimum T (= 270 K) matches that calculated according to the standard 1D isentropic flow theory [10], i.e., $T = 300/(1 + 0.2\, Ma^2)$, (with a specific heat ratio of 1.4 and Ma = 0.746, which yields 269.95 K). Both the ρ field and T field display similar structures as that of the $|U|$ field, with slightly higher density and lower temperature in the high-speed jet velocity region.

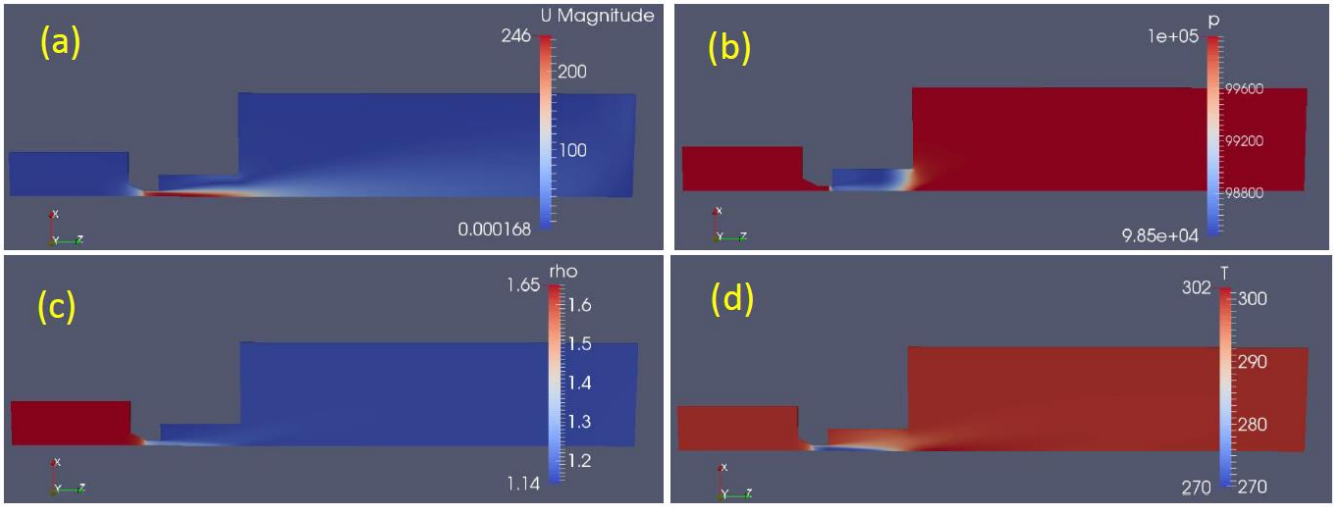

Fig. 3: (a) The field of gas velocity magnitude $|U|$ (m/s), (b) pressure p (Pa), (c) gas density ρ (kg/m^3), and (d) gas temperature T (K) for the nominal case configuration at Q = 1200 sccm.

The profiles of axial velocity component U_z and pressure (in units of bar) are plotted in Fig. 4 as functions of radial distance r (in units of mm), labeled according to the axial distance z (in units of mm) from the exit of jet orifice. At z = 0.5 mm (close to the jet orifice), the U_z profile looks quite similar to that of an incompressible gas jet at the nozzle exit [11], having nearly a plug flow profile with very high shear along the jet edge. As the jet moves away from the orifice, the curves of U_z at z = 1.5 and 2.5 mm show that the edge of the plug flow profile diffuses out while the jet velocity declines with the axial distance. For z < 2.7 mm (within the jet expansion channel), there is a back flow region (as indicated by negative U_z) near the channel wall surrounding the jet as a consequence of mass conservation. The back flow disappears as the free jet moves outside the jet expansion channel into the atomization chamber, where the jet stream widens with further reduced velocity due to viscous diffusion (as seen in experiments [7]).

Also shown in Fig. 4 is a generally positive pressure gradient in the axial direction is consistent with declining jet velocity with z, and the back flow in the jet expansion channel. Each curve shows that the gas pressure generally decreases from jet center with radial distance at a given axial distance z, with a minimum located close to the channel wall where the back flow magnitude is considerably large. So, the lowest pressure does not appear in the region of highest gas velocity at the jet center, according to an intuitive imagination based on Bernoulli's principle. From the fluid dynamics point of view, an expanding gas jet flow is expected to relate to a decreasing pressure in the radial direction; a decreasing jet velocity with axial distance z should correspond to a positive pressure gradient with respect to z, i.e., $dp/dz > 0$. Due to viscous drag, the jet flow tends to bring more gas out of the jet expansion channel than what is supplied from the exit of jet orifice, which creates a reduced local pressure to drive the back flow for compensating the jet depleted gas. Thus, a region of negative pressure appears in the jet expansion channel.

Even out of the jet expansion channel at z = 3.5 and 5.0 mm, a negative pressure about 20 Pa appears near the radial distance r = 0.75 mm and about 5 Pa near r = 1.2 mm, respectively. Such a negative pressure around the jet was sometimes used to suck smoke generated by a nearby smoke wire for the jet flow visualization experiments [9]. Near the jet center, the pressure is higher at z = 3.5 mm with higher gas velocity than that at z = 5.0 mm, while the central pressure generally exhibits lower value with higher jet speed inside the jet expansion channel.

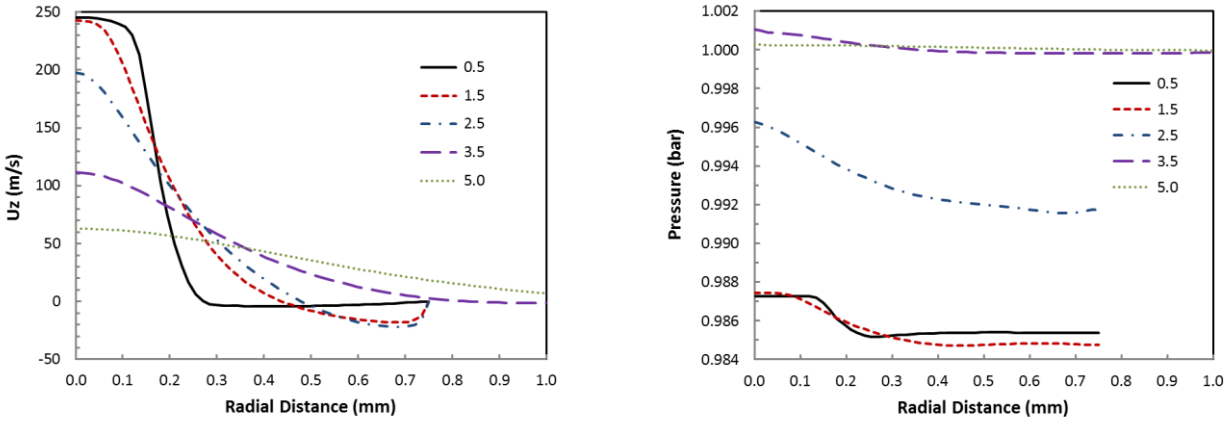

Fig. 4: Radial profiles of axial velocity component U_z and pressure p in the nominal configuration for Q = 1200 sccm at axial distance z = 0.5, 1.5, 2.5, 3.5, 5.0 mm from the exit of jet orifice.

Table 1 shows the CFD results for maximum jet velocity U_{max} and its corresponding Mach number Ma_{max}, the value of negative pressure ΔP (defined as the pressure value at the wall of jet expansion channel 1.5 mm from the exit of jet orifice subtracted from the atomization chamber pressure 10^5 Pa = 1 bar), the gauge pressure upstream to the jet orifice P_g (= p_{max} – 1.0 bar where 1 bar = 10^5 Pa), and minimum gas temperature in the jet flow T_{min}, at various gas flow rates. Those values were found to vary by a few percent with changing of meshing parameters and numerical scheme settings.

Interestingly, with a gas flow rate of Q = 600 sccm the present CFD model indeed predicts a negative pressure of ΔP ~ 380 Pa in most part of the jet expansion channel, consistent with expected minimum values estimated based on hydrostatic pressure and capillary effect as well as empirical knowledge. Also consistent with the theoretical expectation as well as measurements of various pneumatic atomizers [1][4], the value of 'air pressure' P_g increases monotonically with the gas

flow rate Q though the correlation is not exactly linear.

Table 1: Computed values for the nominal case.

Q (sccm)	U_{max} (m/s)	Ma_{max}	ΔP (Pa)	P_g (bar)	T_{min} (K)
600	136	0.397	378	0.111	291
900	194	0.576	862	0.241	281
1200	246	0.746	1524	0.425	270
1500	291	0.903	2218	0.662	258
1800	329	1.046	2755	0.927	246

The magnitude of negative pressure obviously increases with the jet velocity and Mach number Ma. For a jet flow with $Ma < 1$, the structure of subsonic gas flow field remains more or less the same as that shown in Fig. 3 and Fig. 4. When the jet velocity exceeds that of sound, i.e., for $Ma > 1$, the jet flow no longer varies smoothly and rather displays shock wave structures. For Q = 1800 sccm with Ma_{max} = 1.046, a small shock wave zone (with local pressure ~3450 Pa below the ambient value 10^5 Pa) appears right at the exit of the jet orifice. Interestingly, the 1D isentropic flow theory would suggest a local pressure of 3600 Pa below the ambient value.

3.2. Variations with Jet Orifice of D = 0.35 mm

If the nominal case configuration is modified with the diameter of jet expansion channel reduced to D_e = 1.0 mm (from the nominal 1.5 mm), the computed values of U_{max}, Ma_{max}, ΔP, P_g, and T_{min} at various gas flow rates become those in Table 2. Such a reduction of D_e tends to enhance ΔP in the jet expansion channel by a factor of more than 3, with slightly increased jet velocity and Ma_{max} at a given Q. Conversely, with increasing D_e to 1.7 mm (from 1.5 mm) the peak jet velocity for Q = 1200 sccm is reduced from 246 to 244 m/s with Ma_{max} = 0.741, and ΔP becomes 828 Pa, much lower than 1524 Pa with the nominal configuration.

Table 2: As in Table 1 but for reduced expansion channel diameter.

Q (sccm)	U_{max} (m/s)	Ma_{max}	ΔP (Pa)	P_g (bar)	T_{min} (K)
600	138	0.403	1359	0.099	291
900	199	0.592	2904	0.221	280
1200	256	0.780	4946	0.401	267
1500	306	0.958	7377	0.639	253
1800	354	1.136	10052	1.017	241

If the jet expansion channel length L_e is varied by reducing L_e from 2.7 to 2.2 mm, with computed value of ΔP becomes 839 Pa for Q = 1200 sccm. Thus shortening the jet expansion channel length tends to reduce the magnitude of negative pressure. Conversely, increasing L_e to 3.0 mm (with D_e = 1.5 mm) could increase ΔP to 1987 Pa with Q = 1200 sccm. The reason for enhanced negative pressure by shrinking D_e and increasing L_e is simply that a narrower and longer channel corresponds to a greater pressure gradient for driving the same amount of back flow, to compensate the jet depleted gas in the jet expansion channel.

4. Conclusion

From the presented CFD results, a general idea can be gained about the magnitude of negative pressure generated with the compressible gas jet flow in the jet expansion channel of a pneumatic atomizer (as variations of the Collison nebulizer). Whether the value of such a negative pressure ΔP can account for the observed behavior of pneumatic atomization deserves an in-depth discussion.

According to the description of May [1] with measurements of a Collison nebulizer, the typical liquid aspiration rate is about Q_{ink} = 67 ml/min (per jet) for water. This requires an extra pressure difference of about 180 Pa over the ink syphon

tube with a length of L_s = 20 mm and diameter of D_s = 1.5 mm, assuming a liquid viscosity of μ_{ink} = 1.0 cp (= 0.001 Pa s) in the Poiseuille equation for $\Delta p = 128\ \mu_{ink}\ L_s\ Q_{ink} / (\pi D_s^4)$. Including the hydrostatic pressure (200 Pa for ρ_{ink} = 1.0 g/cc), a total negative pressure of magnitude ΔP = 380 Pa (as might be obtained with a gas flow rate of Q = 600 sccm) should be sufficient for syphoning water up at a rate of 67 ml/min. However, the gas flow rate used with the Collison nebulizer was typically Q > 2000 sccm [1] (likely to be with ~2400 sccm at P_g = 20 psig according to the measurements of Niven and Brain [4]), which is expected to produce much more negative pressure (e.g., ΔP > 3000 Pa in view of Table I) than needed for just water aspiration. Hence, the syphoning rate of water is likely restricted by the amount of water accumulated in the jet expansion channel due to limited water removal rate by the blowing gas stream. There must be a dynamic balance between the liquid aspiration rate and the liquid removal rate in the jet expansion channel, for a sustainable continuous atomization. Data from rigorous measurements [4] indeed show an increase followed by a decrease in the liquid aspiration rate (in units of ml/min) with increasing air pressure P_g (or gas flow rate Q) for several "air-jet" nebulizers, while all nebulizers tested show declining trends of liquid aspiration rate in units of "ml per liter of air" with increasing air flow rate (for Q > 2 L/min).

On the other hand, most inks used in the Aerosol Jet® pneumatic atomizer usually have viscosity μ_{ink} > 100 cp (and some may even reach 1000 cp), more than two orders of magnitude greater than that of water and dilute aqueous solutions used by May [1], Niven and Brain [4]. For a comparable aspiration rate, syphoning the Aerosol Jet® inks would require a ΔP > 18000 Pa on top of the hydrostatic pressure (about 400 Pa), which does not seem possible with a gas flow rate Q < 2000 sccm (in view of Table 1). In realistic atomizer operation, however, the flow field in jet expansion channel is not a simplified single-phase gas flow as computed here; instead there is a rather complicated two-phase gas-liquid flow. If we take into account of the fact that part of the jet expansion channel would be filled with the syphoned liquid, the channel volume for gas-phase flow is reduced and the channel diameter effectively shrinks in a dynamic process of liquid being syphoned in and blown out. Reducing the diameter of jet expansion channel due to liquid holdup therein tends to enhance the negative pressure for syphoning (as shown in Table 2), to produce an appropriate liquid aspiration rate. Thus, a dynamic balance of liquid holdup can be imagined as the more liquid syphoned into the channel the more liquid will be blown out for atomization.

At the minimum gas flow rate (e.g., Q = 600 sccm or so) for atomization, the magnitude of negative pressure ΔP may only reach the threshold to bring liquid ink up to the jet expansion channel, with little extra for sustaining the expected liquid aspiration rate in the syphon tube (e.g., > 10 ml/min, as typically measured with various "air-jet" nebulizers [4], corresponding to > 10 cm/s average liquid flow velocity in a syphon tube of 1.5 mm diameter). But as the liquid accumulates in the channel, the channel diameter shrinks and the magnitude of negative pressure increases, leading to greater liquid aspiration rate until a dynamic balance in the liquid holdup is established with the liquid removal rate. Thus, the Collison nebulizer operates with a self-regulating mechanism such that its mist output may not be overly sensitive to the liquid properties such as viscosity, etc.

The amount of liquid holdup in the jet expansion channel is expected to increase with the gas flow rate, up to a certain amount. Beyond an optimal value of the gas flow rate, at which the maximum output mist density is obtained, the liquid aspiration rate as well as subsequent mist generation rate cannot increase proportionally to the gas flow rate; further increasing gas flow rate effectively dilutes the mist even with more liquid being atomized. This could explain why the mist density output from the Collison nebulizer typically goes up and then down as the gas flow rate increases.

Acknowledgements

The author would like to thank Dr. Andreas Mack of TNO Heat Transfer and Fluid Dynamics (Netherlands) for friendly sharing his knowledge in compressible turbulent flow modeling, Mr. Dan Bachman and Mr. Dominick Carluccio of CH Technologies for carrying out intellectually inspiring experimental tests with various configurations of pneumatic nebulizers, and many Optomec colleagues for valuable technical discussions.

References

[1] K. R. May, "The Collison nebulizer: description, performance and application," *J. Aerosol Sci*., vol. 4, pp. 235-243, 1973.

[2] Optomec, *Aerosol Jet Technology*. [Online]. Available: https://www.optomec.com/printed-electronics/aerosol-jet-technology/
[3] J. Q. Feng, "Multiphase flow analysis of mist transport behaviour in Aerosol Jet® system," *Int. J. Comput. Meth. Exp. Meas*., vol. 6, pp. 23-34, 2018.
[4] R. W. Niven and J. D. Brain, "Some functional aspects of air-jet nebulizers," *Int. J. Parmaceut*., vol. 104, pp. 73-85, 1994.
[5] D. R. Hess, "Nebulizers: principles and performance," *Respiratory Care*, vol. 45, pp. 609-622, 2000.
[6] *OpenFOAM README for version 2.4.x*. [Online]. Available: https://github.com/OpenFOAM/OpenFOAM-2.4.x
[7] P. O'Neill, J. Soria, and D. Honnery, "The stability of low Reynolds number round jets," *Exp. Fluids*, vol. 36, no. 3, pp. 473-483, 2004.
[8] V. Todde, P. G. Spazzini, and M. Sandberg, "Experimental analysis of low-Reynolds number free jets: Evolution along the jet centerline and Reynolds number effects," *Exp. Fluids*, vol. 47, no. 2, pp. 279-294, 2009.
[9] C. Gau, C.H. Shen, and Z.B. Wang, "Peculiar phenomenon of micro-free-jet flow," *Phys. Fluids*, vol. 21, p. 092001, 2009.
[10] B. J. Cantwell, Fundamentals of Compressible Flow. [Online]. Available: https://web.stanford.edu/~cantwell/AA210A_Course_Material/
[11] J. Q. Feng, "Sessile drop deformations under an impinging jet," *Theor. Comput. Fluid Dyn*., vol. 29, pp. 277-290, 2015.
[12] A. H. Lefebvre, *Atomization and Sprays*. New York: Hemisphere, 1989.